Quest Journals
Journal of Research in Environmental and Earth Sciences
Volume 7 ~ Issue 7 (2021) pp: 12-32
ISSN(Online) :2348-2532
www.questjournals.org

Research Paper

Rock Attributes for Reservoir Discrimination Using Lame's Parameters

EBONG, S. T.*[1]; EKONG, U. N.[1]; JOSHUA, E. O[2]; AKPABIO, G.T[3]; EFIANG, J.A[1] ATTAI, E. S[4], and EKANEM, K. R[5]

Scientific Research Group (SRG)
[1]*Department of Physics, Akwa Ibom State University, Ikot Akpaden, Akwa Ibom State, Nigeria, (Member SRG).*
[2]*Department of Physics, University of Ibadan, Ibadan, Nigeria, (Member SRG).*
[3]*Department of Physics, University of Uyo, Uyo, Akwa Ibom State, Nigeria, (Member SRG).*
[4]*Department of Physics, Collage of Art and Science, Ikono L.G.A, Akwa Ibom State, Nigeria. (Member SRG).*
[5]*Department of Physics, Akwa Ibom State Polytechnic, Ikot Osurua, Akwa Ibom State, Nigeria, (Member SRG).*
**Correspondents e-mail address: sirphysicsonline@gmail.com*

ABSTRACT
Integrated 3-D Seismic and Well Log Data of Soku field, Niger Delta, was investigated with the aim of identifying reservoir rocks from qualitative interpretation of subsurface seismic view of Soku field acoustic impedance inversion analysis in some selected reservoirs of the field, to derive elastic rock attributes such as Lame's parameters terms (λρ and μρ), Vp/Vs ratio, P-Impedance, S-Impedance from available petrophysical data obtained from the field, rock properties and attributes that better discriminate the reservoir were generated through model based inversion process. Five rock attributes were derived from the data set, inversion of the post-stack seismic data was also carried out to generate acoustic impedance volumes; V_P/VS-Ratio, I_P, I_S, λρ and μρ volumes. Data slices of the inverted acoustic impedance volumes were then generated to observe the wells locations along hydrocarbon charged sands, wet sands or shales channels. Three wells were analysed and attributes generated. The inversion results; in figure 14 to 18 estimate the P-impedance (I_P), S-impedance (I_S), V_P/V_S-ratio, Lame' parameters (μρ – Mu-rho and λρ – lambda-rho) that discriminate lithology/fluids contrast related to hydrocarbon charged sands and wet sands; the P-wave/Gamma ray curve is bounded by at the top of SOKU-3000 on the inverted volumes with the lowest values of V_P/V_S-Ratio (1.8338), I_P (6265), λρ (6.1), and μρ (19.9) and table 1 are indicative of hydrocarbon (gas) charged sands and the gas saturation is detected at the depth interval of 10428-10525m (97m) in Soku-2. Based on these observations, seismic inversion of the post-stack seismic data can be used as good indicator of lithology, pore fluid contrasts and to predict presence of hydrocarbon accumulation in the porous gas and oil sands.

KEYWORDS: *Hydrocarbon, Inversion, Rock attribute, reservoir and Seismic*

Received 06 July, 2021; Revised: 18 July, 2021; Accepted 20 July, 2021 *Published with open access at www.questjournals.org*

I. INTRODUCTION

A reservoir is a porous permeable formation which is capable of containing trapped hydrocarbon in its in-situ conditions and releasing same when penetrated by wells during production. The objectives of reservoir characterization are to identify reservoirs, delineate them, and subsequently determine the distribution of relevant physical properties such as lithology, porosity, permeability, water saturation and pore pressure, which will make for an easy determination of the reservoirs economic potential (Dopkin and Wang, 2008).

Seismic amplitudes are usually observed on seismic sections due to contrasts in elastic rock properties at the interface between two geologic layers. Rock properties are those physical properties of a rock, which can affect the way seismic wave travel through the rock. They include P-wave velocity (Vp), S-wave velocity (Vs), density (ρ), and their attributes (which is a simple combination of the rock properties), P- and S- impedances (Zp and Zs), Poisson's ratio (ν) and incompressibility (λρ) and shear modulus (μρ) (Dewar, 2001).

Quantitative interpretation of pre-stack seismic-inversion attributes has become industry standard and is essential both in prospect mapping during hydrocarbon exploration and in reservoir characterization during appraisal and production. There are several different approaches but the common goal of all the methods is to extract information about lithology, reservoir quality, and pore fluids from the prestack seismic amplitudes for

reservoir characterization (Chopra and Castagna, 2014). The onshore Niger Delta has gradually assumed the status of a matured oil and gas producing province. A lot of bypassed reservoirs could still be won from these old oilfields using newer approaches. One of such tools is rock physics/seismic inversion and one of its primary goals is to enhance the understanding of the physical properties of the reservoir. Usually, at the location of a drilled well, we have measurements that give us a good idea of the elastic and physical properties of the subsurface rocks (Velocity, Density, Lithology, Porosity, etc.). However, to understand these properties away from the well, we have to rely on seismic data volumes. Rock physics studies now help us to link these properties to the seismic data and infer their variation in a lateral and vertical sense (Sayers and Chopra, 2009). In effect, by studying the physical rock properties at known hydrocarbon bearing intervals at well locations, one can use the results to delineate other potential hydrocarbon zones away from wells.In this study, the key deliverable is to integrate rock physics and seismic data inversion to predict rock and fluid properties, for reservoir characterization of parts of the Niger Delta away from existing wells so as to create new exploration and development opportunities in the field (Udo, K.I...*et al* 2017).

II. LOCATION OF THE STUDY AREA

Soku field is located in the coastal swamp of the Niger Delta, some 40km north of the present day coastline and about 40km southwest of Bayelsa State as shown below in figure1. Niger Delta basin is situated at the southern end of Nigeria boarding the Atlantic Ocean and extends from about longitude 3^0E to 9^0E and latitude 4^0N to 5^0N.

Figure 1: *Map of the study location*

The Niger Delta is perhaps the most important sedimentary basin in sub-Sahara African due to its petroleum production, and it is one of the most important deltas in terms of its geology which is unique and classical as shown in figure 2.

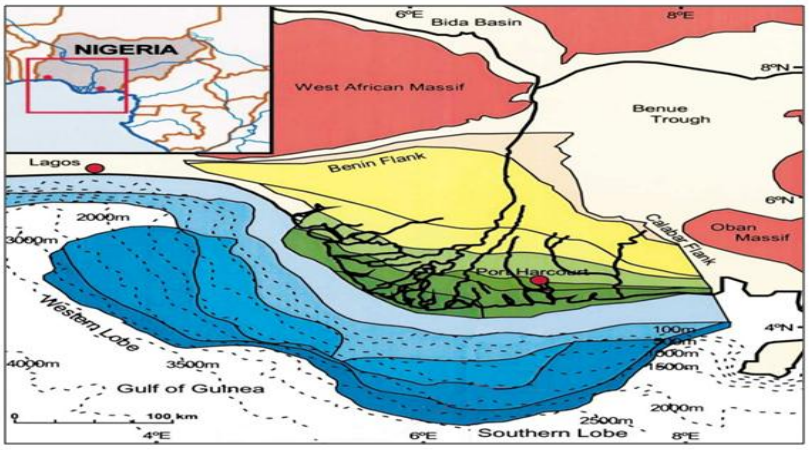

Figure 2: *Location map of the Niger Delta showing the depobelts and geologic features that bounds the delta (Tuttle et al., 1999).*

Regional geologic setting: The onshore portion of the Niger Delta where the coastal swamp depobelt is situated is delineated by the geology of southern Nigeria and south-western Cameroon (Figure 2). The northern boundary is the Benin flank, an east-northeast trending hingeline south of the West Africa basement massif. The north-eastern boundary is defined by outcrops of the Cretaceous on the Abakiliki High and further east-southeast by the Calabar flank, a hinge line bordering the adjacent Precambrian. The offshore boundary of the Niger Delta is defined by the Cameroon volcanic line to the east, the eastern boundary of the Dahomey basin to the west, and the two-kilometre sediment thickness to the south and southwest (Figure 2). The province covers 300 000km^2 and includes the geologic extent of the Tertiary Niger Delta (Akata-Agbada) Petroleum System (Tuttle *et al.* 1999).

III. THEORETICAL FRAMEWORK:

Deterministic and model based approach to inversion: Burianyk (2000), observed that the display sections obtained from the linearized Zoeppritz equations of P- and S- impedance reflectivity (Fatti *et al.*, 1994) was more robust than those of P-normal incidence and gradient reflectivity (Shuey, 1985). The author further used the P- and S- reflectivities obtained from Fatti approximation to extract the P- and S- impedance through post-stack rock property inversion, which were in turn combined into rock properties of Lambda-Rho and Mu-Rho. The Lambda- Rho and Mu-Rho display showed low values of Lambda-rho (incompressibility) and relatively unchanged values of Mu-rho (rigidity) for both gas sands. Using Lambda-Rho and Lambda / Mu ratio derived from pre-stack data corresponding to the stacked section of real seismic data, combining both $\lambda\rho$ *and* $\lambda\rho/\mu\rho$ ratio in cross plot clearly showed only two of the wells had gas and the other two were wet sands. Bachrach *et al.* (2004), presented a general workflow for 3D lithology analysis and prediction by combining rock physics, full waveform pre-stack inversion and high resolution seismic interpretation, with a case study from the Gulf of Mexico. Seismic-scaled probability density function were generated from petrophysical analysis, rock physics analysis and seismic inversion for elastic attributes, and used in the Bayesian classification. Al-Khaled *et al.* (2006), presents the result of the application of rock physics analysis, seismic data inversion, multi-attribute analysis and neural network to help optimise new water flood project in a reservoir from a single sensor land 3D survey. The paper showed that the inverted acoustic impedance improved the interpretation with strong relationship between acoustic impedance, effective porosity and water saturation. Pendrel (2006) reiterates the relevance of seismic inversion as an effective tool in reservoir characterization. The paper posited that quantitative rock properties derived from inversion facilitates better estimation of reservoir properties such as porosity and net pay.

Generalized fluid method for impedances: Russell *et al.* (2003) proposed the generalized fluid method by using Biot-Gassmann theory. They reformulated the equation for P-wave velocity using a fluid term and skeleton term. These give more intuitive insight into the effect of pore fluid on the bulk modulus and P-wave velocity.

Under the low frequency assumption, the incompressibility and bulk modulus for the saturated porous sandstone can be expressed as the sum of the dry term and fluid term (Biot, 1941, and Gassmann, 1951):

$$\lambda_{sat} = \lambda_{dry} + \beta^2 M \quad \text{and} \qquad (1)$$

$$K_{sat} = K_{dry} + \beta^2 M \qquad (2)$$

where $\beta^2 M$ is the contribution of the pore fluid. β measures the ratio of the volume change in the fluid to the volume change in the formation when hydraulic pressure is constant (Russell *et al.*, 2003).

From equation 1, Gassmann further showed that

$$\beta = 1 - \frac{K_{dry}}{K_{matrix}} \qquad (3)$$

$$\frac{1}{M} = \frac{\beta - \phi}{K_{matrix}} + \frac{\phi}{K_{fluid}} \qquad (4)$$

Gassmann's pore space modulus *M* is defined as the pressure needed to force water in the formation without changing the volume (Russell *et al.*, 2003).

Substituting equation 2 and equation 3 into equation 1, the equation for P-wave velocity for the saturated porous rock can be written as:

$$V_p = \sqrt{\frac{\lambda_{dry} + 2\mu_{dry} + \beta^2 M}{\rho_{sat}}} = \sqrt{\frac{K_{dry} + {}^4/_3 \mu_{dry} + \beta^2 M}{\rho_{sat}}} \qquad (5)$$

that is,

$$K_{eff} = \rho_{sat} V_p^{\,2} =$$

$$K_{dry} + 4/3\,\mu_{dry} + \frac{1-(K_{dry}/K_{matrix})^2}{(1-\phi-K_{dry}/K_{matrix})/K_{matrix}+\phi/K_{fl}} \qquad (6)$$

Dry rock (skeleton, s) — fluid term (f)

or more concisely,

$$\rho_{sat} V_p^{\,2} = s + f \qquad (7)$$

Similarly, $\rho_{sat} V_s^{\,2} = \mu_{dry}$ (8)

where, s = $K_{dry} + 4/3\,\mu_{dry}$= Skeleton term (9)

and f = $\frac{1-(K_{dry}/K_{matrix})^2}{(1-\phi-K_{dry}/K_{matrix})/K_{matrix}+\phi/K_{fl}}$ = Fluid term (10)

Equation 5 shows the fluid term and the skeleton term in the P-wave equation. The fluid term can be estimated using P-wave impedance and S-wave impedances. To extract the fluid term, the equations for P-wave impedance and S-wave impedance can be reformulated as:

$$Z_p = \rho V_p = \sqrt{\rho(f+s)} \quad (11)$$

and $Z_s = \rho V_s = \sqrt{\rho\mu}$ (12)

Using equation 11 and 12, the following function can be constructed:

$$Z_p^{\,2} - cZ_s^{\,2} = \rho(s+f-c\mu) = \rho f \quad (13)$$

Equation 12 shows that the constant *c* is defined by the term of P-wave and S-wave velocities for dry rocks or the elastic modulus for the dry rock. For different reservoirs, the value of the constant *c* will vary with lithology, shale content, and temperature. The value of *c* can be derived from wellbore rock samples for the local reservoir interval.

Equation 12 can be reformulated as:

$$\rho f = Z_p^{\,2} - cZ_s^{\,2} = (Z_p + \sqrt{c}Z_s)\,(Z_p - \sqrt{c}Z_s) \quad (14)$$

When c=2; $\lambda\rho = \rho f$

The difference term in the above equation is much more sensitive than the sum term to differentiate the fluid content. This difference-term is the same as the fluid factor ΔF proposed by Smith and Gidlow (1987). The fluid term ρf estimated from the generalized fluid method using *c*=2 is equal to $\lambda\rho$ which can be derived from LMR method (Goodway *et al.,* 1997). $\lambda\rho$ represent changes coming from combination of fluid and rock skeleton. The fluid term $\lambda\rho$ gives good discrimination between hydrocarbon bearing porous sandstones and shales.

Recall: $\lambda\rho = (Z_p + \sqrt{c}Z_s)\,(Z_p - \sqrt{c}Z_s)$ (15)

Quakenbush *et al.,* (2006) introduced the concept of Poisson Impedance (*PI).* This is a portion of the difference of two squares expression of the Lamda-Rho concept (equation 14) of Goodway *et al.,* 1997.

Equation 13 can be rewritten as $\lambda\rho$ = PI $(Z_p + \sqrt{c}Z_s)$ (16)

IV. MATERIALS AND METHOD

Data sets used: Well logs and seismic data from SOKU field were analysed using Hampson Russell Software (HRS). The well log data was evaluated, seismic and rock attribute cross-sections were created.

Well log importation: Three wells from Soku field were imported for the well log analysis and model based inversion process. This provides the much needed low-frequency component. The wells give insight into the various formation measured properties. The importation of the well data was done through the use of eLog application of the HRS in addition to their tops (SOKU-3000) and check-shot corrections. The suite of wireline log data imported comprises of caliper log, gamma ray log, resistivity log, density log and sonic log. The inverse of the interval transit times of the sonic logs were used to generate the compressional velocities for each well. We generated S-wave data from Castagna´s relation using P-wave for well that did not have S-wave log. As shown in figure 7a,b,c and 12.

Check – Shot Correction: Check-shot correction was carried out in all wells in both fields with respect to each well calibrated with individual well velocity shot as shown figure 4 the corrections show in each well, the input depth/time curve (black), the output sonic log (red with light solid line), corrected time curve (red curve with points plot) and drift curve (blue curve with points plot).

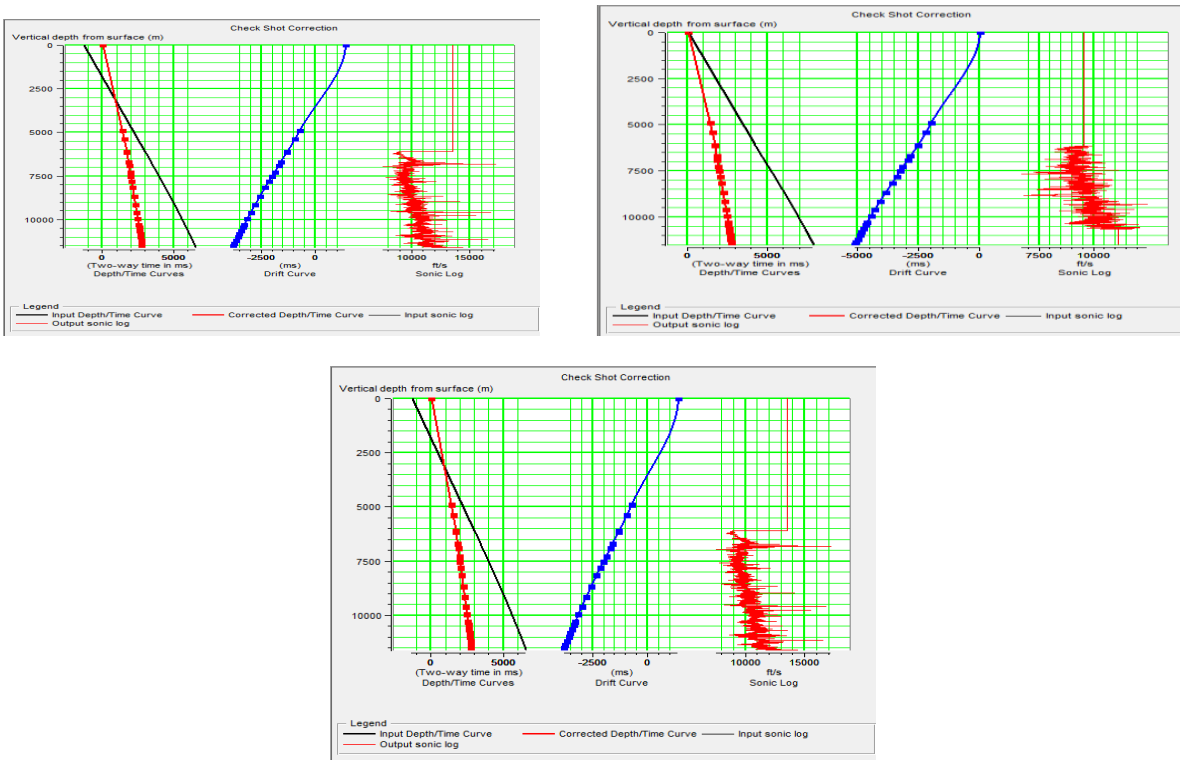

Figure 4: *Check shot correction applied and analysis window in all wells (Soku field).*

Seismic Data Importation: The post stack seismic data (full – Soku field) used for the acoustic impedance inversion typically model based inversion was imported through the Seismic Loader/Strata window of Hampson Russel software as shown in the geometry figure 5 and 6a,b,c.

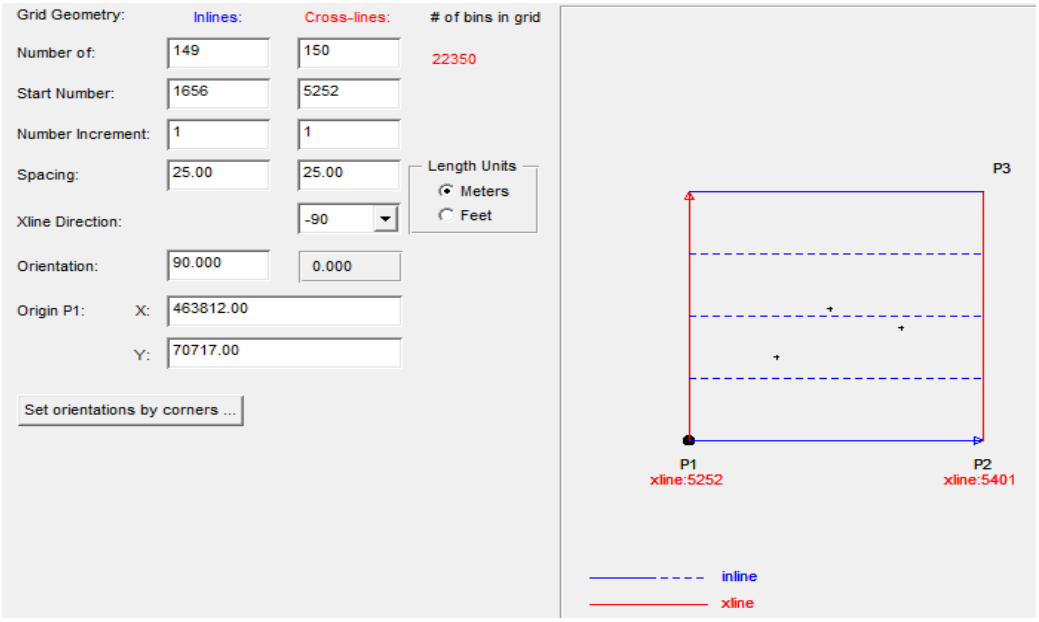

Figure 5: *Shows the Soku fields inlines and crosslines grid geometry with the following loading parameters; orientation – 90.00 (rectangular shape with plot of three wells), Xline Direction -90, Length units in meters, Spacing 25.01 – Inline and 25.00 – Xline. Start number: Inlines (1659) and Cross lines (5252-5401).*

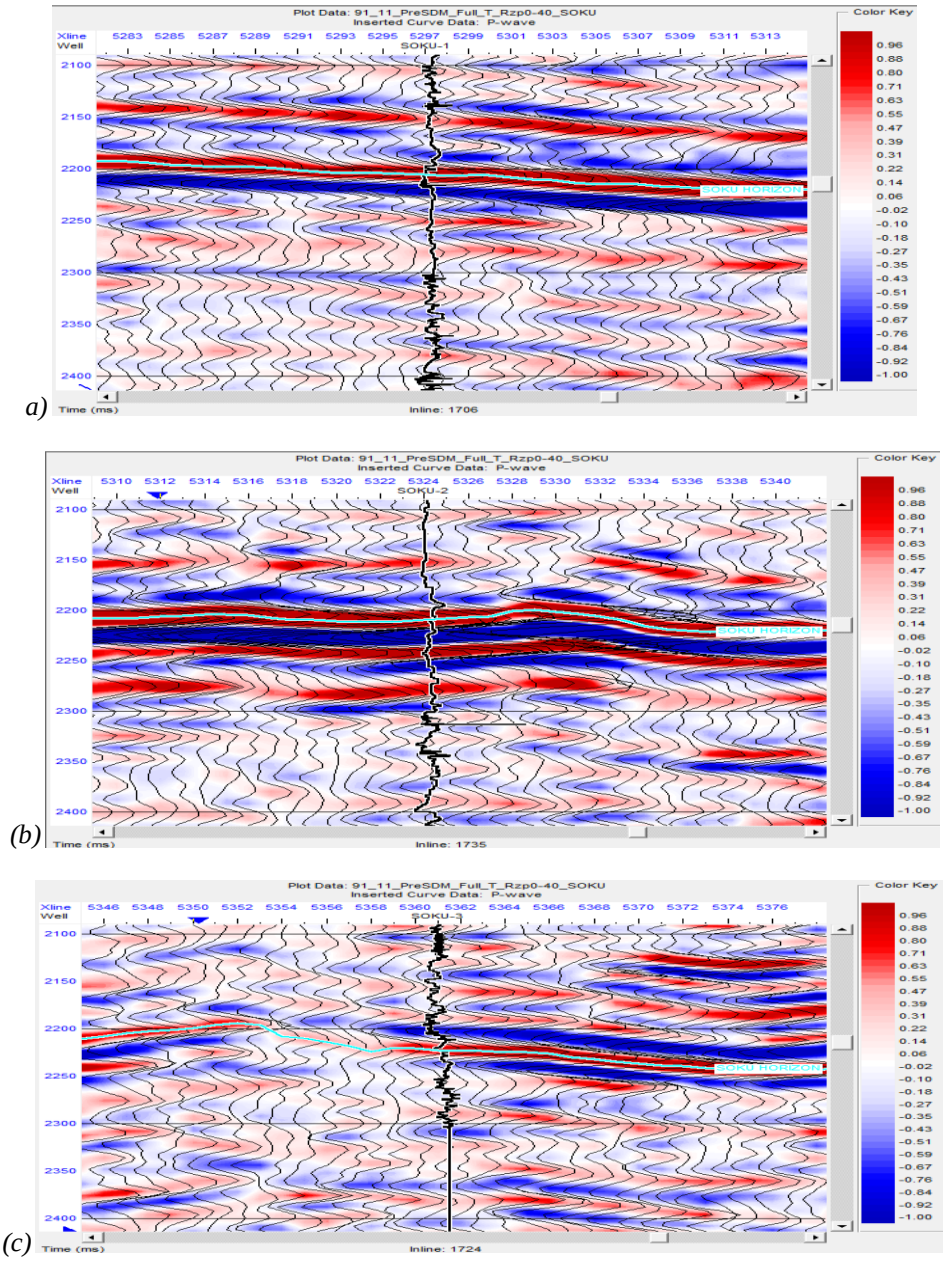

a)

(b)

(c)

Figure 6a,b,c: Inline and Cross line *seismic section of Soku field between 2100 – 2400ms showing P-wave log at each well inline and xline numbers and picked Horizon across the top of SOKU-3000 reservoir expected.*

Well and Seismic Correlation: Correlation is basically a measure of the similarity between a pair of traces. In the study, after extraction of statistical wavelet (Zero - phase) which was based on measuring the autocorrelations of the seismic data and assuming that the earth reflectivity is "white" (has zero autocorrelations at non-zero lags) and a small check shot correction applied, a good tie (correlation coefficient = 86%) was achieved between seismic trace and synthetic seismogram using well stretching technique in Strata windows as in figure 7a, b and c.

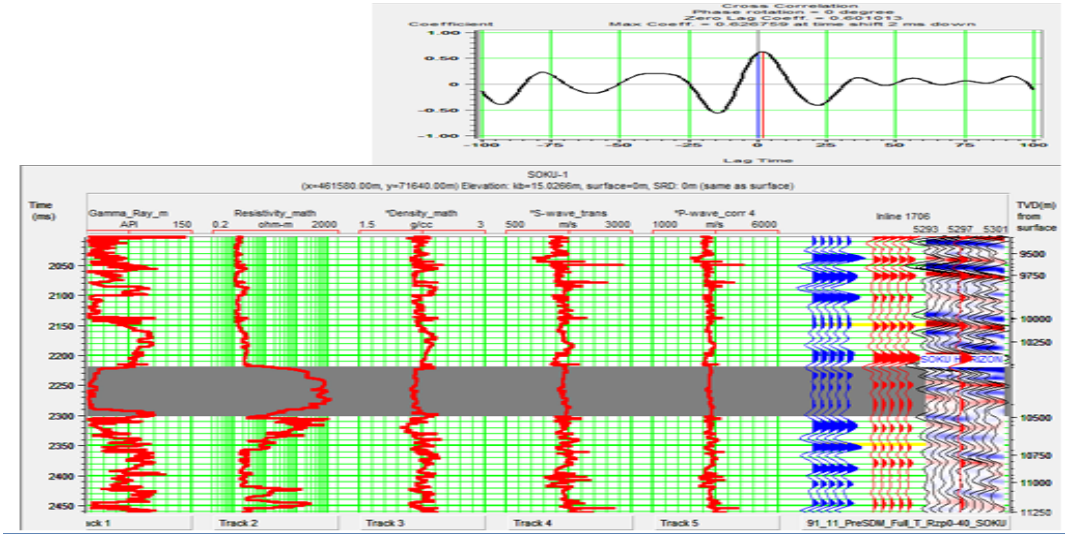

Figure 7a: *Log correlation for well Soku-1 showing the synthetic seismic generated from wavelet and well data (blue traces) and sampled seismic data close to the well (red) and a correlation co-efficient of 60% with a time lag of 2ms in which Soku Horizon spreads across the SOKU-3000 reservoir top.*

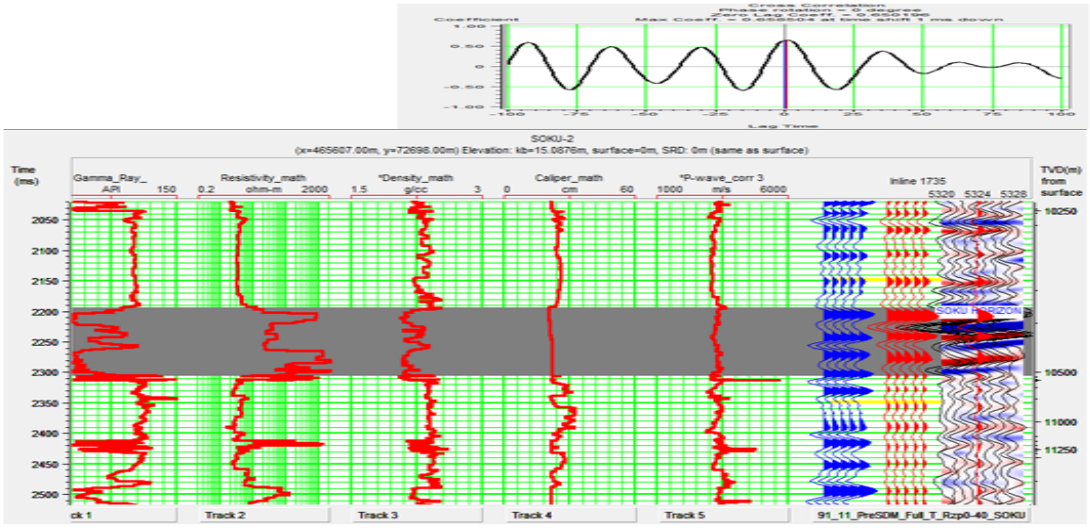

Figure 7b: *Log correlation for well Soku-2 showing the synthetic seismic generated from wavelet and well data (blue traces) and sampled seismic data close to the well (red) and a correlation co-efficient of 65% with a time lag of 1ms in which Soku Horizon spreads across the SOKU-3000 reservoir top.*

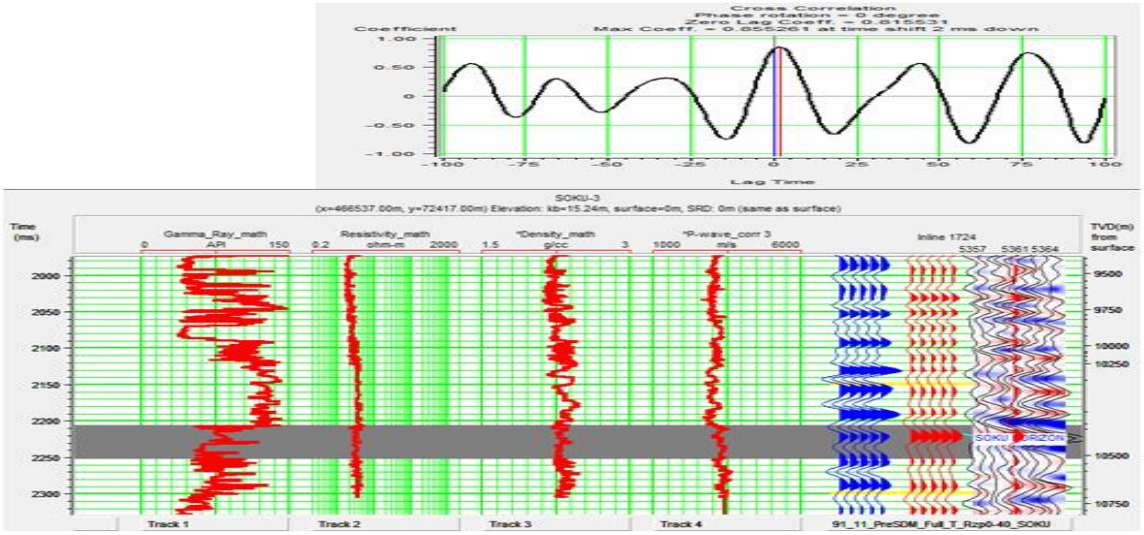

Figure 7c: *Log correlation for well Soku-3 showing the synthetic seismic generated from wavelet and well data (blue traces) and sampled seismic data close to the well (red) and a correlation co-efficient of 80% with a time lag of 2ms in which Soku Horizon spreads across the SOKU-3000 reservoir top.*

Picking Horizons: There were two main methods of getting horizons into Strata window where 3D data inversion is performed; importation of horizons or picking of horizons. Of these two, importation is usually preferred. But the field of study had no horizon. Thus, the second method was used (picking horizon across the full seismic stack volume in the field. Horizons are very important in the process because they act as a priori information for the building of the initial model. The final volume of inverted data takes its structure from the initial horizon that was picked across the initial model as showing in figure 8.

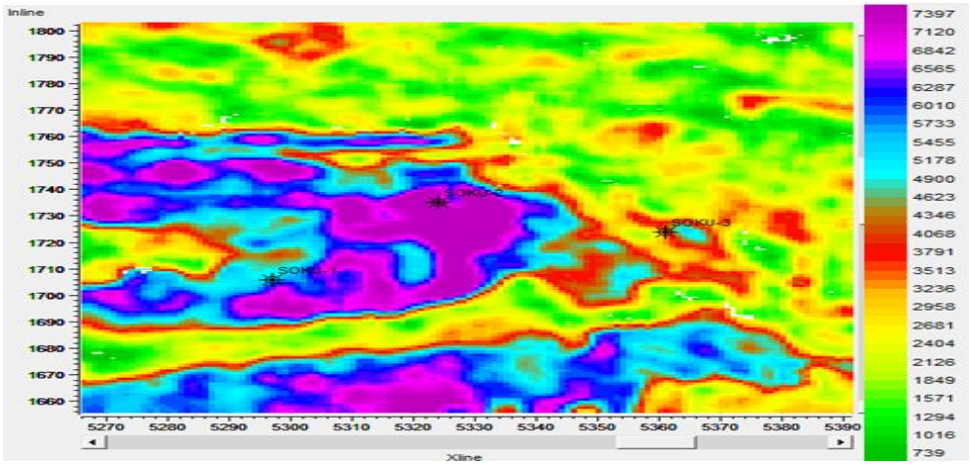

Figure 8:*Soku field Horizon automatically picked at 2212 ms across the seismic section between the In-line (1656-1804), Cross-line (5252-5401) showing the plot of three wells at low time reflector (Soku-3) high time reflectors (Soku-1 and 2)*

Initial Model: The initial model for the model based inversion was built using the Strata interface. An option with an advanced setup was chosen using the data available (P-Impedance log, S-Impedance log, Vp/Vs log, Mu-rho and Lambda-rho logs). These are the logs required for the typical setup for an initial model of any seismic rock attributes. The most recent of the edited logs were set as the active logs for the purpose of the initial model. The logs were combined with the picked horizons to control the interpolation and to provide structural information for the model between the wells in the area in order to obtain initial AI- model and others. The cross-sections in figure 9 show the initial acoustic impedance model in the field.

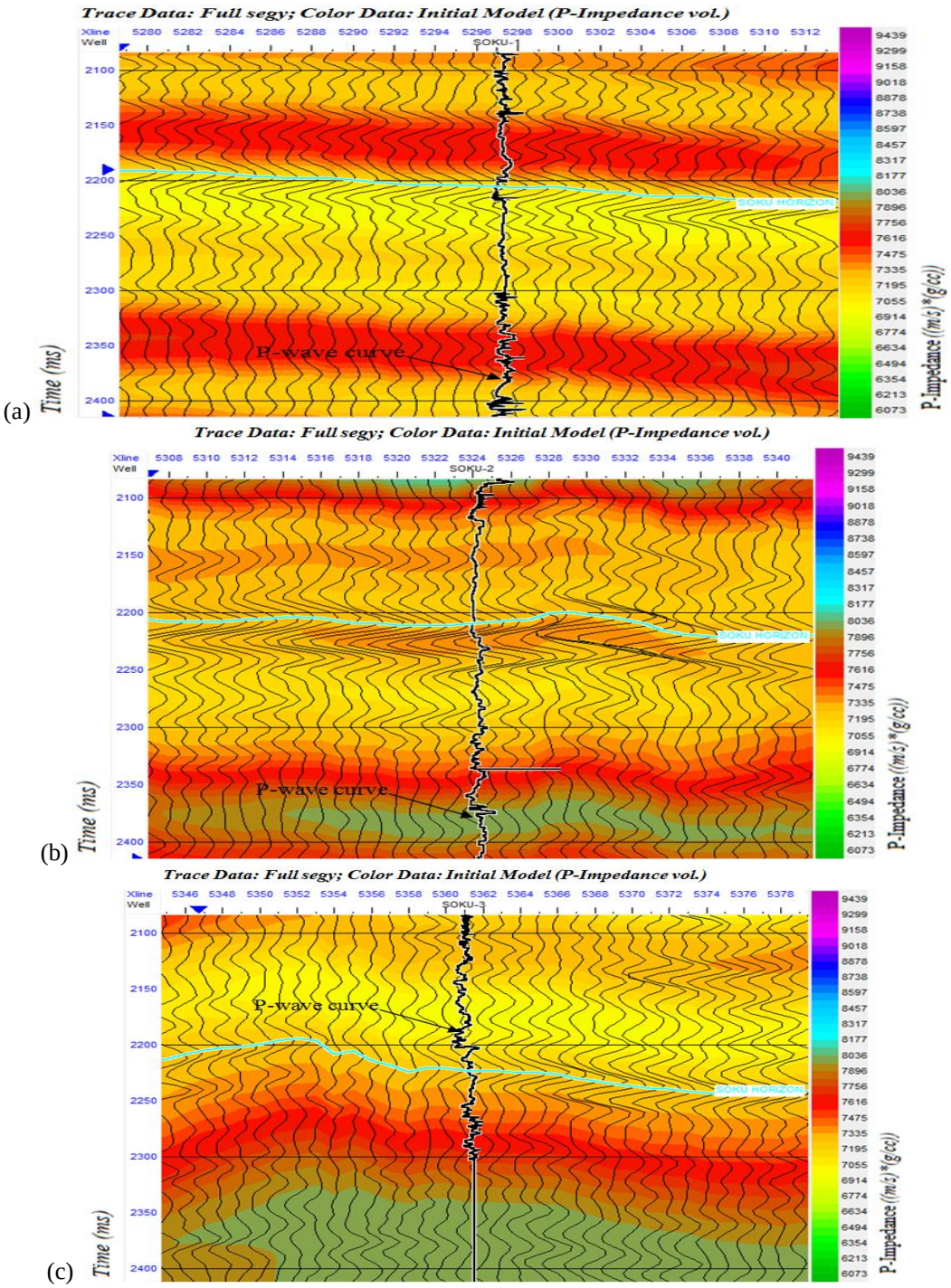

Figure 9:a,b,c; Cross-line view of *seismic section (full segy)superimposed with color section (initial model-P impedance) of Soku field between 2100-2400ms showing P-wave log plot at each well inline and xline numbers and picked Horizon across the top of SOKU3000 reservoir expected where low P-wave log is bounded by low section of initial model.*

V. DATA ANALYSIS, RESULT AND DISCUSSION

Well Log Analysis: The curves used for the analysis are well logs of Soku-1, 2 and 3 from the field of study as shown in figure 11. The logs include gamma ray overlay with caliper log, density, P- wave, S-wave, Porosity and Water Saturation logs. The true vertical depth (TVD) of each well ranges from 6126m to 11600 m, 6875m to 12100m and 6100m to 12000m for Soku-1, Soku-2 and Soku-3 respectively. The reservoir of interest analyzed is SOKU-3000 with thickness of 10400-10500m (Soku-1), 10428-10525m (Soku-2) and 10423-10516m (Soku-3) which are present in the three wells in field as shown in figure 12. However, the wells exhibit a dominantly shale/sand/shale sequence typical of the Niger delta formation. The wells were analysed in terms

of fluid type and lithology within the zones of interest in which Shale lithologies were delineated by the high gamma ray (Shale lithologies cause the deflection of Gamma curve to the right) and resistivity to the far left due to its high conductive nature. Sand lithologies deflect the Gamma ray curve to the left and Resistivity curve to the far right indicating probable hydrocarbon charged sand. Thus, Regions showing low gamma ray, high resistivity, high porosities and low water saturation are mapped (circled) as sand lithologies with probable hydrocarbon zone in each well as shown in figures below. On the other hand, regions showing high gamma ray, low resistivies, low porosities and high water saturation are mapped as shale lithologies.

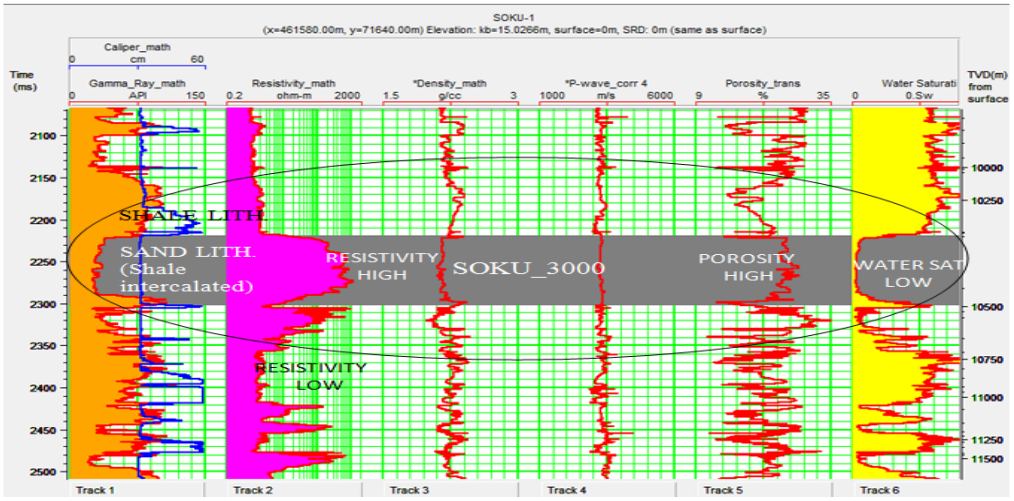

Figure 11a: *Soku-1 suite of logs used in the analysis; low-Gamma ray, high-Resistivity, low-Density, low-P-wave, high-Porosity and low-Water Saturation with SOKU-3000 having a thickness of 10400-10500m (100m).*

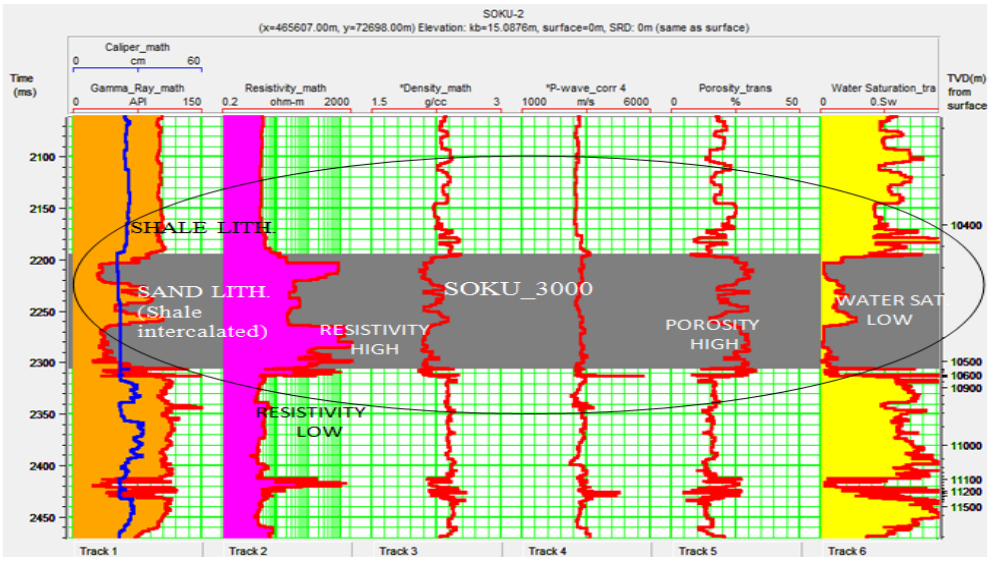

Figure 11b: *Soku-2 suite of logs used in the analysis; low-Gamma ray, high-Resistivity, low-Density, low-P-wave, high-Porosity and low-Water Saturation with SOKU-3000 having a thickness of 10428-10525m (97m).*

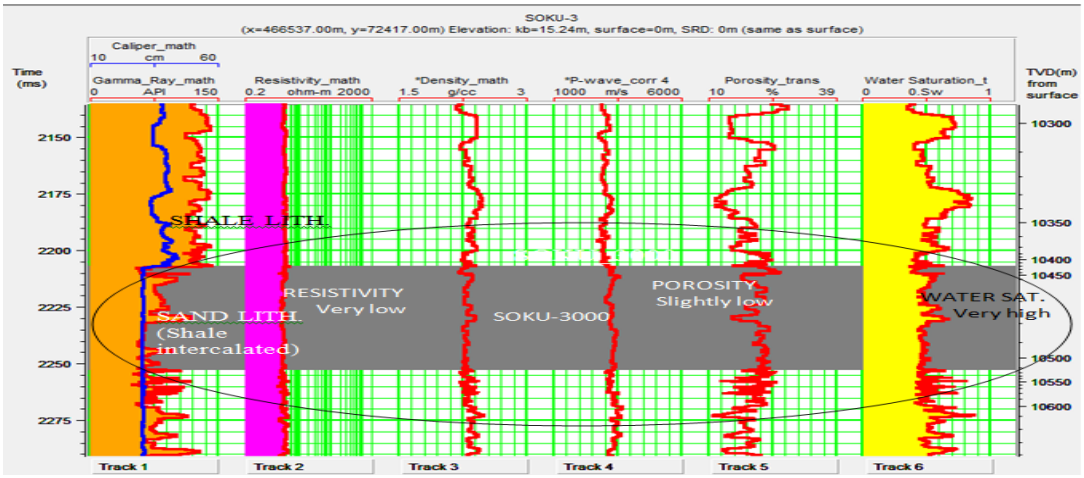

Figure 11c: *Soku-3 suite of logs used in the analysis; low-Gamma ray, no change in (Resistivity, Density, P-wave, Porosity and Water Saturation) with SOKU-3000 having a thickness of 10423-10516m (93m).*

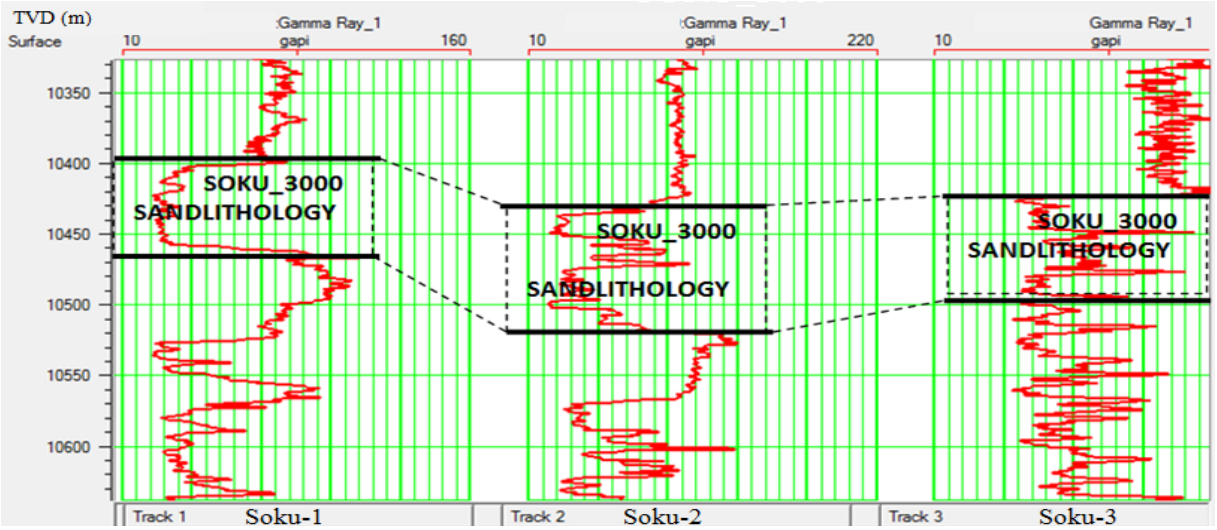

Figure 12: *Correlation of sand lithologies (SOKU-3000) in Soku fields using Gamma ray curves as guide*

Seismic Inversion Attributes Analysis: For reservoir characterization of Soku-field ''SOKU-3000''; the post stack seismic volumes of the field were inverted to estimate the P-impedance (I_P), S-impedance (I_S), V_P/V_S-ratio, Lame' parameters (μρ – Mu-rho and λρ – lambda-rho) that further discriminate lithology/fluids contrast related to hydrocarbon charged sands and wet sands.

P- Impedance (I_p) Cross-Section: Figure 14 (Soku field) show the inverted P-impedance cross-section superimposed with 3D seismic volumes (Full Segy = full seismic exploration geophysics) from time window of 1800-2050 ms and 2100-2400ms. There is a good match between the I_P features distribution, seismic wiggles and the P-wave log (P-wave log is the black curve in the Inverted P-impedance cross section plotted at In-line and Xline: 1706, 5297; 1735, 5324; 1724, 5361 for Soku-1, 2 and 3 respectively, the highest I_P values (8.457 – 9.439 $*10^3$m/s × g/cc, blue and purple) correspond to Soku shales. Intermediate acoustic impedance values (7.335 – 8.317 $*10^3$m/s × g/cc, red and cyan) correspond to Soku wet sands. The lowest I_P values (6.073 – 7.195 $* 10^3$ m/s × g/cc, green and yellow) are associated with Soku hydrocarbon charged sands. However, Soku Horizon are indicative of the top of SOKU-3000 reservoirs on inverted section which show that these regions are bounded by low P-impedance due to hydrocarbon presence. The horizontal time slice (amplitude map) – figure 14(d) – for Soku-field extracted from P-impedance shows the hydrocarbon charge sands , wet sands and shales channels in which the highest I_P values (7.505-8.015 $* 10^3$ m/s x g/cc, blue and purple) correspond to shales reflector, intermediate I_P values (6.921-7.432 $* 10^3$ m/s x g/cc, red and cyan) correspond to wet sands reflector, and the lowest value of I_p (6.265-6.848 $* 10^4$ m/s x g/cc) correspond to hydrocarbon charged sand. Here the wells location exhibits low values of I_p especially in Soku-1 and Soku-2 but high values of I_p in Soku-3 attributed to shales.

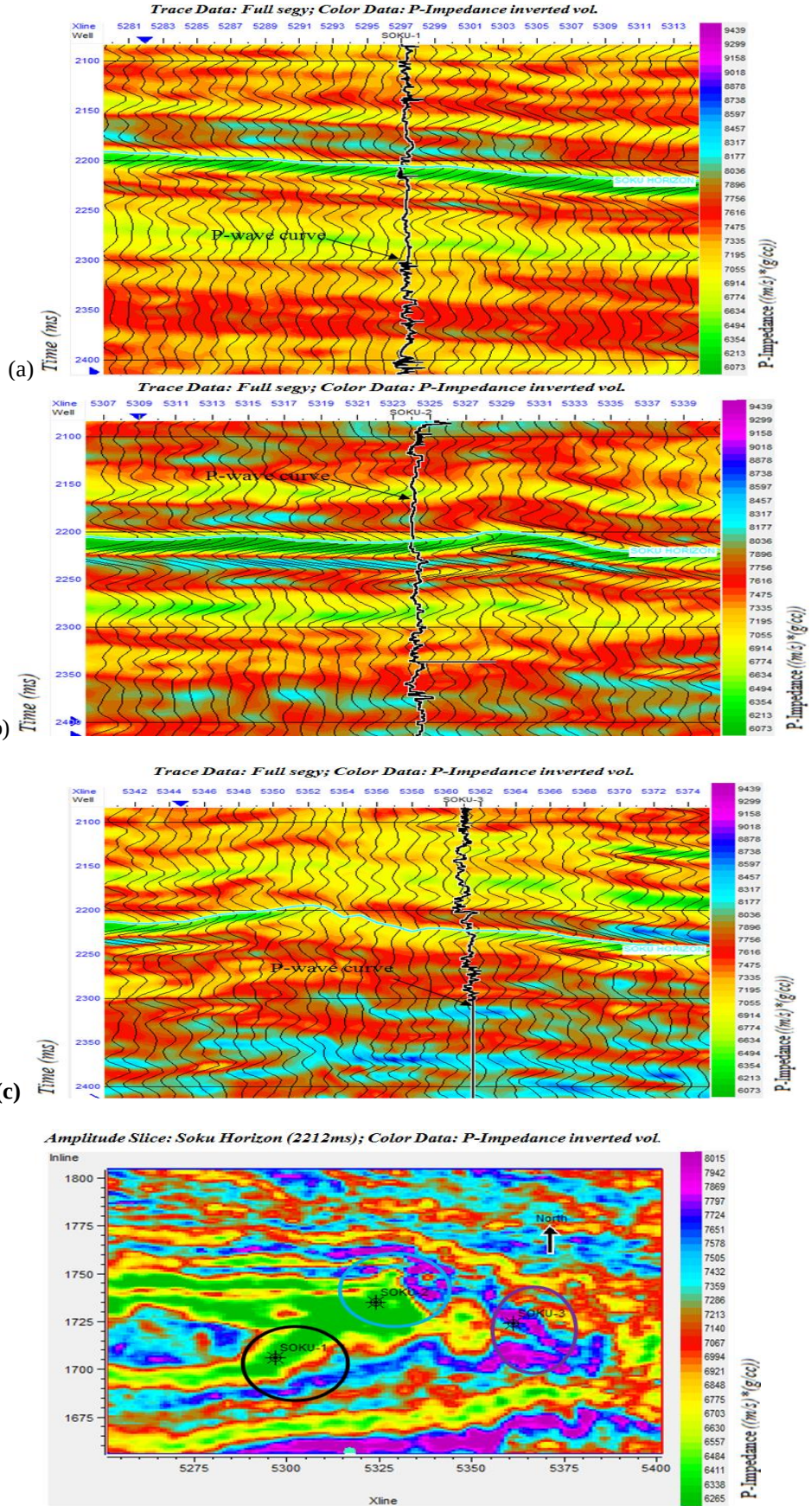

Figure 14: *Soku field inverted I_P corssection; (a) shows Soku-1 Plot, (b) Soku-2 plot, (c) Soku-3 plot and (d) horizontal time slice (Amplitude map).*

V_P/V_S-Ratio Cross-Section: Figure 15 show the inverted V_P/V_S-Ratio cross-section superimposed with 3D seismic volumes (Full Segy) from time window of 1800-2050 ms and 2100-2400ms. There is a good match between the V_P/V_S features distribution, seismic wiggles and the Gamma ray log (Gamma ray log is the black curve in the Inverted V_P/V_S cross section plotted at In-line and Xline: 1706, 5297; 1735, 5324; 1724, 5361 for Soku-1, Soku-2 and Soku-3 respectively. We derive V_P/V_S from Ip and Is. V_P/V_S ratio is used in pore fluid and lithology identification (Ostrander, 1984). The V_P/V_S ratio ($=I_P/I_S$) is a fluid indicator because of compressional waves. The V_P/V_S crossection in figure 15 shows locally high values are sensitive to fluid changes, whereas shear waves are not (except in the special case of very viscous oil; Han *et al.,* 2007). As (2.1503-2.2945, blue and purple) corresponds to Soku shales, intermediate values of V_P/V_S (1.9648-2.1297, red and cyan) correspond to fluids (Oil/Brine) and locally low values of V_P/V_S (1.7999-1.9442, green and yellow) correspond to Gas in the Soku-field sandstone. However, Soku Horizon are indicative of the top of SOKU-3000 reservoirs on inverted section which show that these regions are bounded by low V_P/V_S-Ratio due to hydrocarbon presence. The horizontal time slice (amplitude map) figure 15(d) for Soku-field extracted from V_P/V_S shows the hydrocarbon charge sands , wet sands and shales channels in which the highest V_P/V_S values (2.2253-2.3967, blue and purple) correspond to shales reflector, intermediate V_P/V_S values (2.0296-2.2009, red and cyan) correspond to wet sands reflector, and the lowest value of V_P/V_S (1.8093-2.0051, green and yellow) correspond to hydrocarbon charged sand. Here the wells location exhibits low values of V_P/V_S especially in Soku-1 and Soku-2 but high values of V_P/V_S in Soku-3 attributed to shales.

(a)

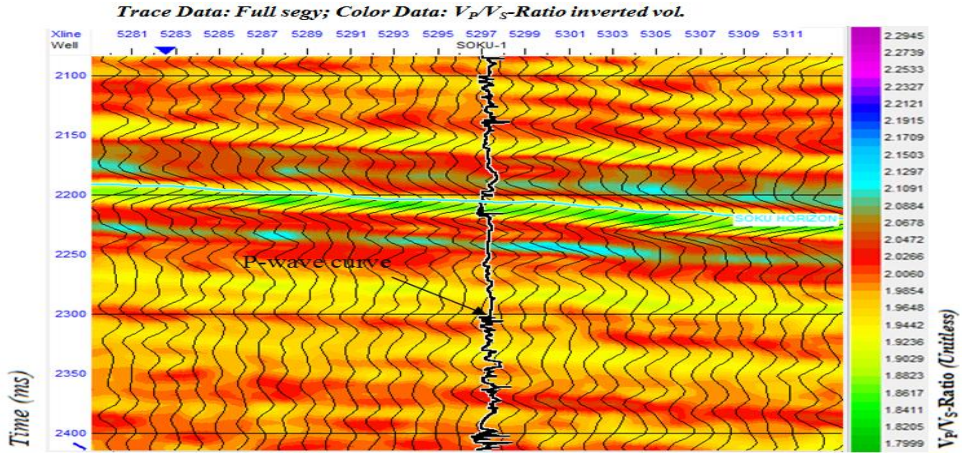

(b)

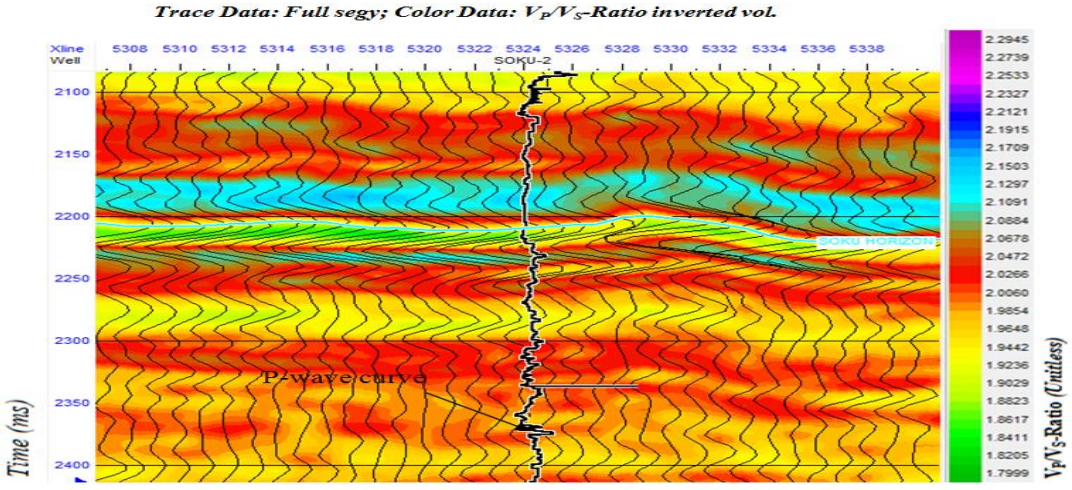

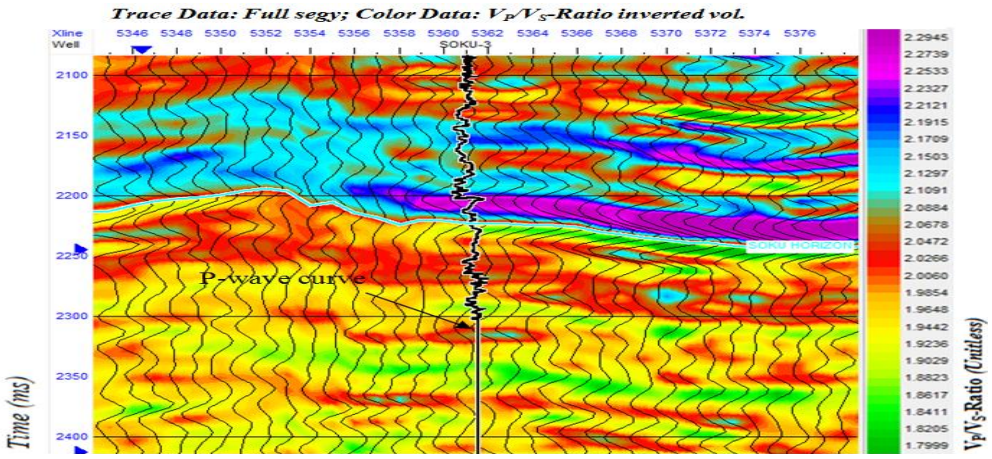

(c)

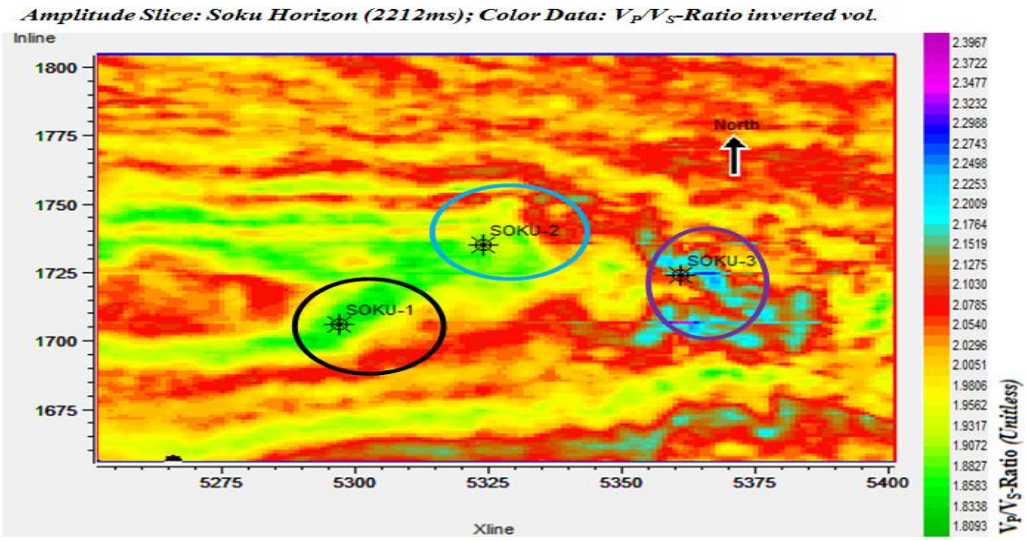

(d)

Figure 15: *Soku field inverted* V_P/V_S *crossection; (a) shows Soku-1 Plot, (b) Soku-2 plot, (c) Soku-3 plot and (d) horizontal time slice (Amplitude map).*

S- Impedance (I_S) Cross-Section: Figure 16 show the inverted S-impedance cross-section superimposed with 3D seismic volumes (Full Segy) from time window of 1800-2050 ms and 2100-2400ms. There is a good match between the I_S features distribution, seismic wiggles and the P-wave log (P-wave log is the black curve in the Inverted P-impedance cross section plotted at In-line and Xline: 1706, 5297; 1735, 5324; 1724, 5361 for Soku-1, Soku-2 and Soku-3 respectively, the highest I_S values (3.937 – 4.587 $*10^3$m/s × g/cc, blue and purple) correspond to Soku shales. Intermediate Shear impedance values (2.962 – 3.829 $*10^3$m/s × g/cc, red and cyan) correspond to Soku wet sands. The lowest I_S values (1.988 – 2.854 * 10^3 m/s × g/cc, green and yellow) are associated with Soku hydrocarbon charged sands. The Soku field Horizon are indicative of the top of SOKU-3000 reservoirs on inverted section which show that these regions are bounded by low S-impedance due to hydrocarbon presence. The horizontal time slice (amplitude map) – figure 16(d), extracted from S-impedance shows the hydrocarbon charge sands , wet sands and shales channels in which the highest I_S values (3.890-4.471 * 10^3 m/s x g/cc, blue and purple) correspond to shales reflector, intermediate I_S values (3.226-7.3.807 * 10^3 m/s x g/cc, red and cyan) correspond to wet sands reflector, and the lowest value of I_S (2.479-3.143 * 10^3 m/s x g/cc) correspond to hydrocarbon charged sand. Here the wells location exhibits low values of I_S especially in Soku-1 and Soku-2 but high values of I_S in Soku-3 attributed to shales.

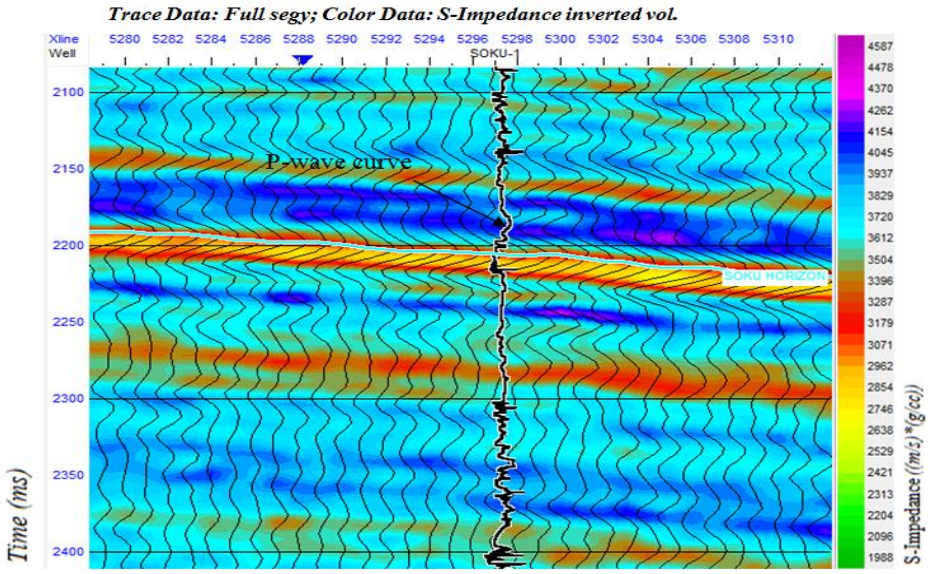
Trace Data: Full segy; Color Data: S-Impedance inverted vol.
Xline
Well
SOKU-1
P-wave curve
SOKU HORIZON
Time (ms)
S-Impedance ((m/s)*(g/cc))

(a)

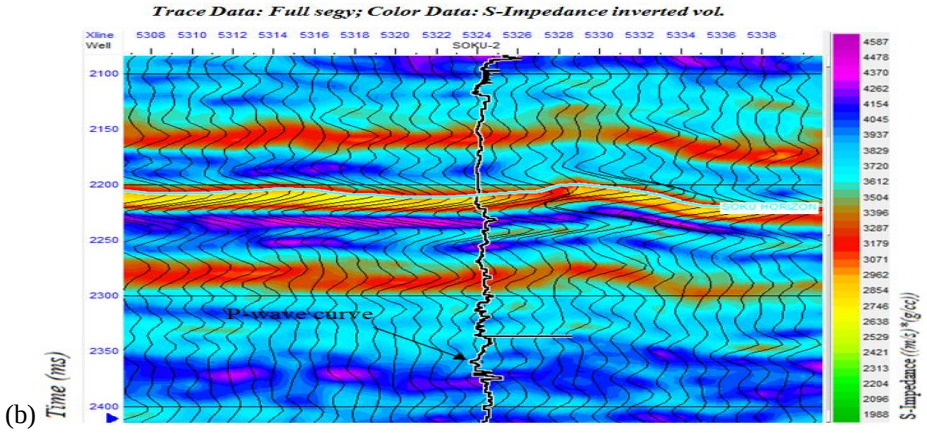
Trace Data: Full segy; Color Data: S-Impedance inverted vol.
Xline
Well
SOKU-2
P-wave curve
SOKU HORIZON
Time (ms)
S-Impedance ((m/s)*(g/cc))

(b)

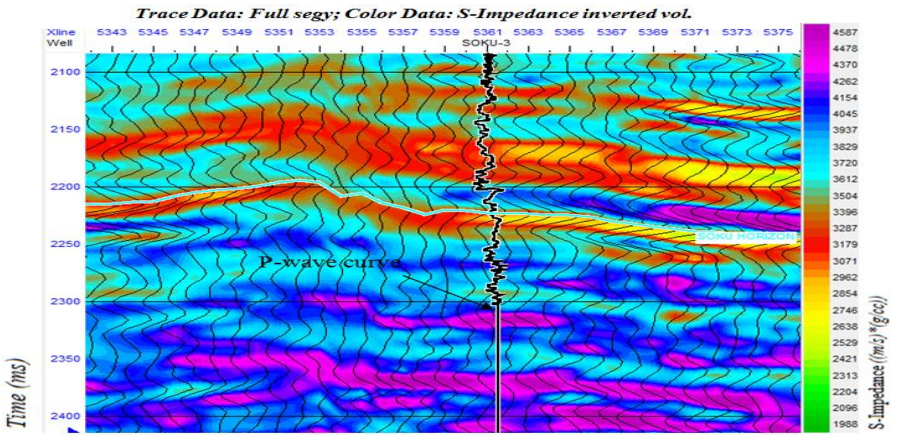
Trace Data: Full segy; Color Data: S-Impedance inverted vol.
Xline
Well
SOKU-3
P-wave curve
SOKU HORIZON
Time (ms)
S-Impedance ((m/s)*(g/cc))

(c)

(d)

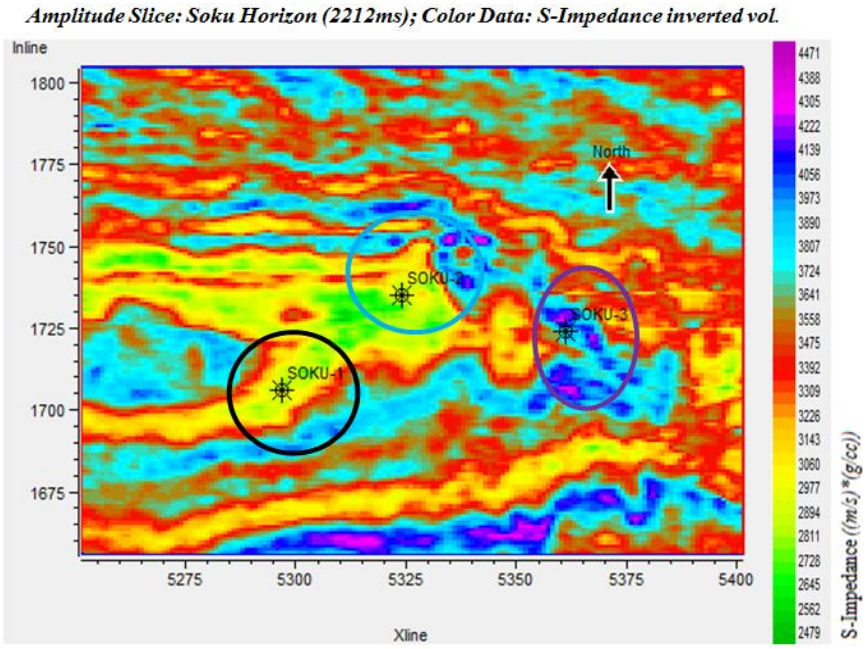

Figure 16: *Soku field inverted I_S crossection; (a) shows Soku-1 Plot, (b) Soku-2 plot, (c) Soku-3 plot and (d) horizontal time slice (Amplitude map).*

Lambda-Rho (λρ) Crossection: Goodway *et al.* (1997) shows that the Lamé parameter terms μρ and λρ are good pore fluid indicators and can be calculated using

$\lambda\rho = I_P^2 - 2I_S^2$ ---------- *

and $\mu\lambda = I_S^2$ ---------- ---------- **

Where the Lamé parameters are λ (which is sensitive to pore fluid) and μ (which is sensitive to matrix connectivity but is independent of the pore fluid) (Dufour *et al*., 2002).

Figure 17 show the inverted Lambda-Rho (λρ) cross-section superimposed with 3D seismic volumes (Full Segy) from time window of 1800-2050 ms and 2100-2400ms. There is a good match between the λρ features distribution, seismic wiggles and the Gamma log (Gamma log is the black curve in the Inverted Lambda-Rho (λρ) cross section plotted at In-line and Xline: 1706, 5297; 1735, 5324; 1724, 5361 for Soku-1, Soku-2 and Soku-3 respectively, the highest λρ values (30.80 – 34.3 GPa × g/cc, blue and purple) are indicative of Soku shales. Intermediate λρ values (26.90 – 30.4 GPa × g/cc, red and cyan) are indicative of Soku oil/brine. The lowest λρ values (22.4 – 26.4 GPa × g/cc, green and yellow) are indicative of Soku Gas. However, Soku Horizon are indicative of the top of SOKU-3000 reservoirs on inverted section which show that these regions are bounded by low λρ due to hydrocarbon presence. The horizontal time slice, figure 17(d) extracted from λρ are indicative of the hydrocarbon charge sands , wet sands and shales channels in which the highest λρ values (29.6-34.1 GPa x g/cc, blue and purple) are indicative of shales reflector, intermediate λρ values (24.4-28.9 GPa x g/cc, red and cyan) are indicative of wet sands reflector, and the lowest value of λρ (18.6-23.7 GPa x g/cc) are indicative of hydrocarbon (Gas) charged sand. Here the wells location exhibits low values of λρ especially in Soku-1 and Soku-2 but high values of λρ in Soku-3 attributed to shales.

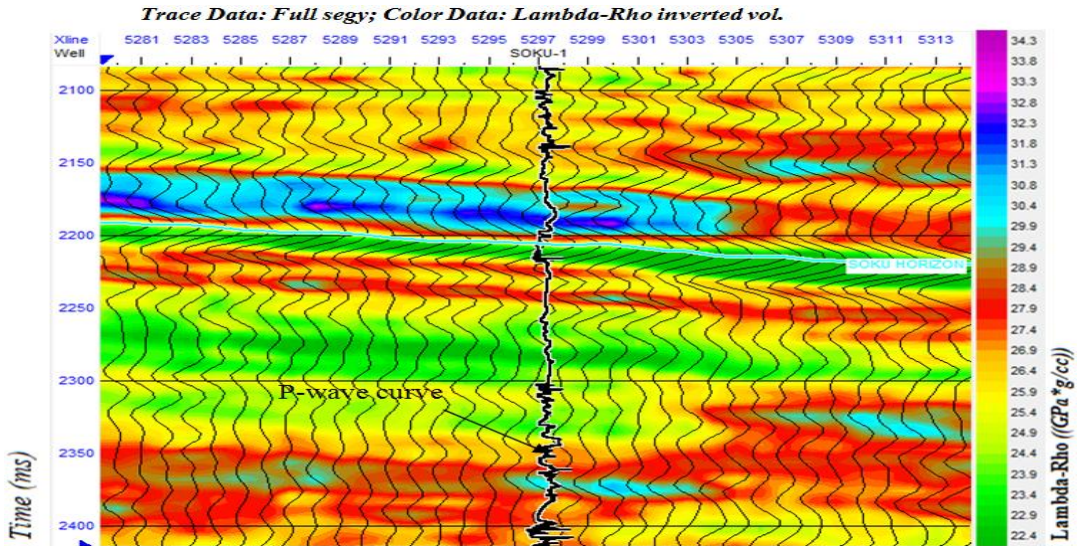
Trace Data: Full segy; Color Data: Lambda-Rho inverted vol.
Xline
Well
SOKU-1
P-wave curve
SOKU HORIZON
Time (ms)
Lambda-Rho ((GPa*g/cc))

(a)

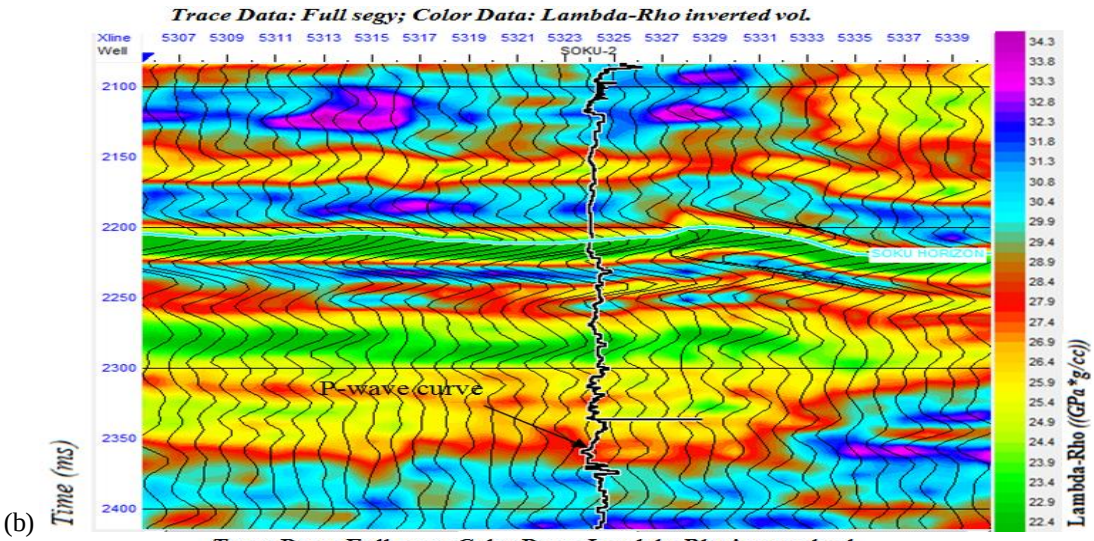
Trace Data: Full segy; Color Data: Lambda-Rho inverted vol.
Xline
Well
SOKU-2
P-wave curve
SOKU HORIZON
Time (ms)
Lambda-Rho ((GPa*g/cc))

(b)

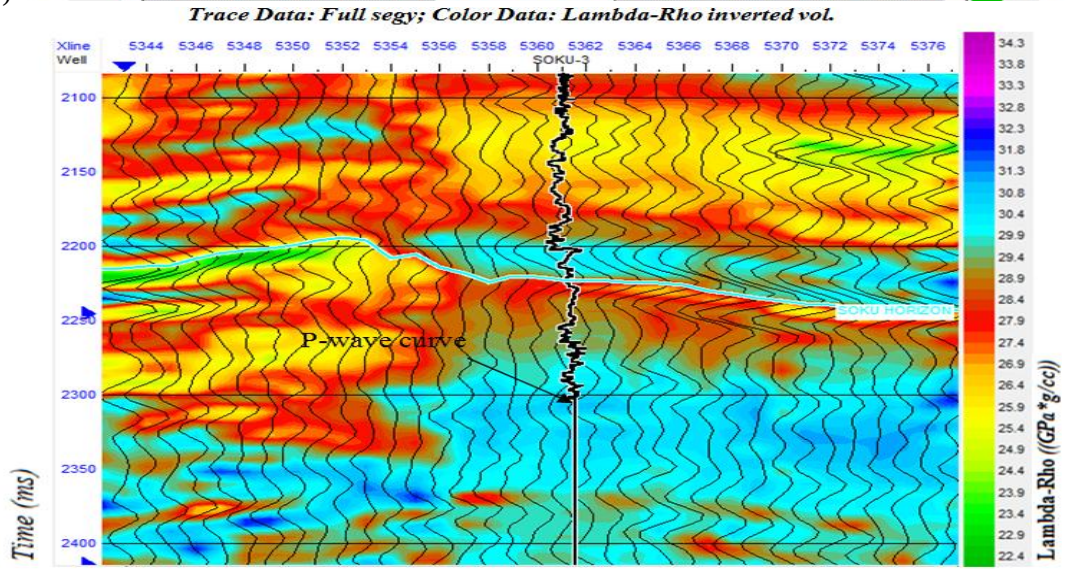
Trace Data: Full segy; Color Data: Lambda-Rho inverted vol.
Xline
Well
SOKU-3
P-wave curve
SOKU HORIZON
Time (ms)
Lambda-Rho ((GPa*g/cc))

(c)

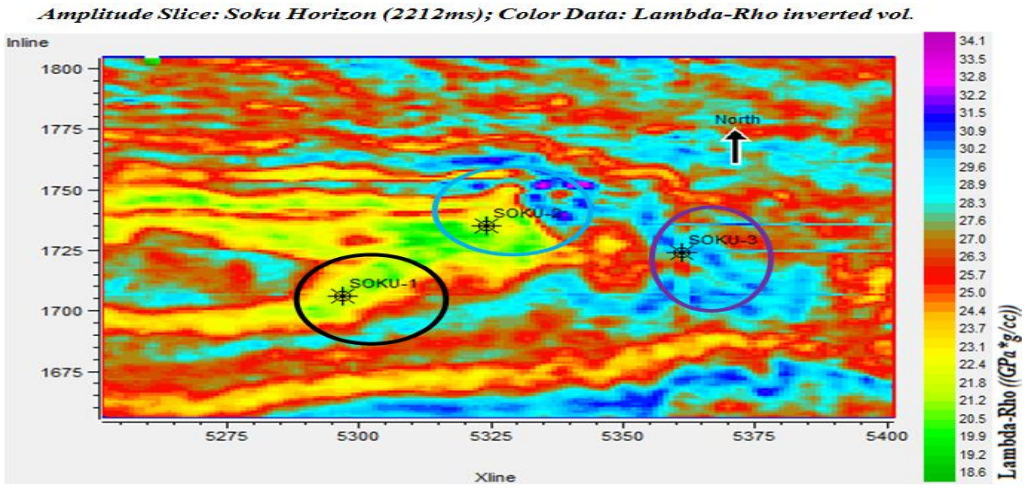

(d)

Figure 17: *Soku field inverted Lambda-Rho(λρ) crossection; (a) shows Soku-1 Plot, (b) Soku-2 plot, (c) Soku-3 plot and (d) horizontal time slice (Amplitude map).*

Mu-Rho (μρ) Cross-section: The Mu-rho attribute gives a quantitative measure of the variation in rigidity and lithology (Goodway and Downton, 1997). Figure 18 show the inverted Mu-Rho (μρ) cross-section superimposed with 3D seismic volumes (Full Segy) from time window of 1800-2050 ms and 2100-2400ms. There is a good match between the μρ features distribution, seismic wiggles and the Gamma log (Gamma log is the black curve in the Inverted Lambda-Rho (μρ) cross section plotted at In-line and Xline: 1706, 5297; 1735, 5324; 1724, 5361 for Soku-1, Soku-2 and Soku-3 respectively. For Soku field, the μρ is a lithology indicator with high values (19.7 – 24.7 GPa × g/cc, blue and purple) indicative of Soku shales. Intermediate μρ values (14.0 – 19.0 GPa × g/cc, red and cyan) indicative of Soku wet sands. The lowest μρ values (7.6 – 13.3 GPa × g/cc, green and yellow) indicative of Soku Gas sand saturation. Soku Horizon are indicative of the top of SOKU-3000 reservoir on inverted section which show that these regions are bounded by low μρ due to hydrocarbon presence. The horizontal time slice figure 18 (d) extracted from μρ are indicative of the hydrocarbon charge sands , wet sands and shales channels in which the highest μρ values (16.0-20.0 GPa x g/cc, blue and purple) indicative of shales reflector, intermediate μρ values (11.3-15.4 GPa x g/cc, red and cyan) indicative of wet sands reflector, and the lowest value of μρ (6.1-10.8 GPa x g/cc) indicative of hydrocarbon (Gas) charged sand. Here the wells location exhibits low values of μρ especially in Soku-1 and Soku-2 but high values of μρ in Soku-3 attributed to shales.

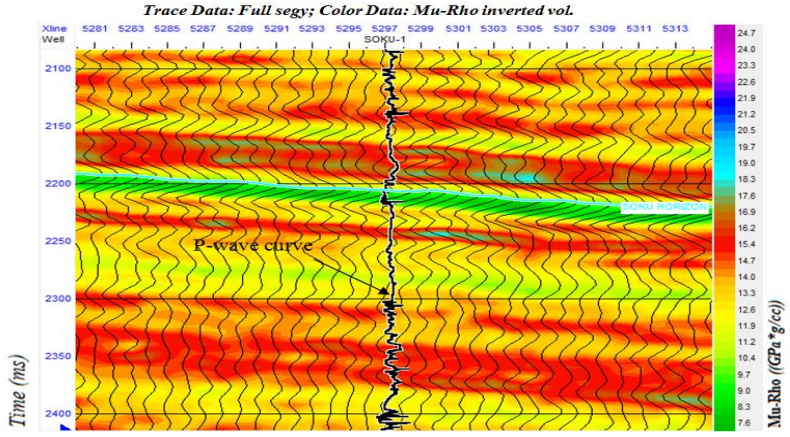

(a)

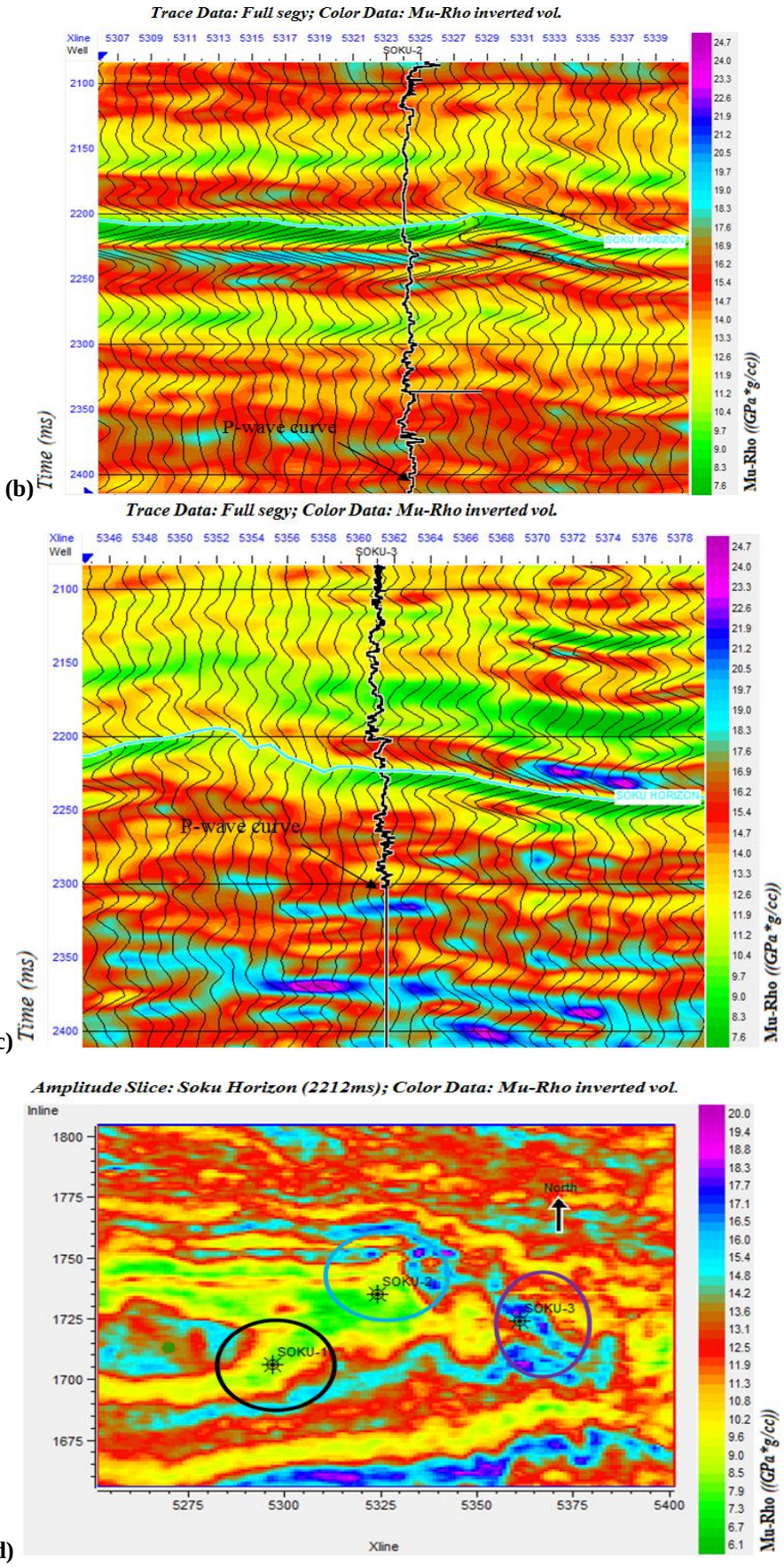

Figure 18: *Soku field inverted Mu-Rho(μρ) crossection; (a) shows Soku-1 Plot, (b) Soku-2 plot, (c) Soku-3 plot and (d) horizontal time slice (Amplitude map).*

Table 1: Showing wells locations in horizontal time slices (Amplitude Maps) of each inverted volume of seismic attributes

Wells location	I_P (m/s*g/cc)	I_S (m/s*g/cc)	V_P/V_S (Unitless)	μρ (GPa*g/cc)	λρ (GPa*g/cc)
Soku-1	6484	2977	1.8583	21.2	7.3
Soku-2	*6265*	*2728*	*1.8338*	*19.9*	*6.1*
Soku-3	7797	4222	2.1519	29.6	18.3

The P-impedance (I_P), V_P/V_S-Ratio, and the lames' parameters (μρ, λρ) were found to be most robust in lithology and fluid discrimination within the reservoirs.

Inversion of 3D post stack seismic data was performed to directly generate acoustic impedance volumes from which rock attributes and petrophyisical properties (V_P/V_S, I_P, I_S, λρ and μρ) were extracted from seismic volumes for comparison in the well log analysis. It is observed that, in Soku-field, figure 14 to18; the P-wave/Gamma ray curve is bounded by at the top of SOKU-3000 on the inverted volumes with the lowest values of V_P/V_S-Ratio (1.8338), I_P (6265), λρ (6.1), and μρ (19.9), table 1, are indicative of hydrocarbon (gas) charged sands. Also the high value of all these parameters might be due to shales/wet sands intercalations. The well and seismic tie reveals that the hydrocarbon charged sands (gas sands Soku-2 SOKU-3000) are associated with low values of seismic attributes on the inverted crossection and wet/shales which could be possible seal or source rock are associated with Soku-3 wells having increase in extracted seismic attributes.

VI. CONCLUSION:

From the analysis, Vp/Vs-ratio, P-impedance, Lamda-rho and Mu-rho attributes were found to be most robust in lithology and fluid discrimination within the reservoir. However, results from λ-μ-ρ inversion provided greater insight into rock properties for pore fluid and lithology discrimination by isolating Lame' impedance parameters (Lambda-Rho (λρ) and Mu-Rho (μρ)) from the seismic reflectivity response. The combined interpretation of Vp/Vs, Ip, Is, Lambda-Rho (λρ) and Mu-Rho (μρ) attributes from the post-stack 3D seismic data enhanced the identification and delineation of hydrocarbon charged sands with greater confidence. Low values of Lambda-Rho (λρ), Vp/Vs, Ip, associated with moderate to high values of Mu-Rho (μρ), indicate the presence of hydrocarbons within the sand reservoir (SOKU-3000). These results now confirm that this approach can be applied with confidence in delineating hydrocarbons sands in mature fields within the Niger Delta basin and thereby increasing production from such fields.

REFERENCES

[1]. Al-Khaled, Q., Al-Zuabi, Y., Rahaman, M., Ai-Jenai, J., and Hussain, T. (2006): Seismic inversion of single sensor land 3D seismic survey: Kuwait Magwa field, Wara reservoir: 76th Annual International meeting, SEG, Expanded Abstract, 2102-2105.

[2]. Bachrach, R., Belier, M., Liu, C.C., Perdomo, J., Shelander, D., Dutta, N., and Benabentos, M. (2004): Combining rock physics analysis, full waveform prestack inversion and high-resolution seismic interpretation to map lithology units in deep water: A Gulf of Mexico case study: The Leading Edge, 04, 378 — 383.

[3]. Biot, M.A., (1941): General theory of three-dimensional consolidation, Journal of Applied physics, 12, 155-164.

[4]. Chopra, S., and J. P. Castagna, 2014, AVO: SEG Investigations in Geophysics Series No. 16, http://dx.doi. org/10.1190/1.9781560803201.

[5]. Dufour, J., J. Squires,W. N. Goodway, A. Edmunds, and I. Shook, (2002): Integrated Geological and Geophysical interpretation case Study, and Lamé Rock Parameter Extractions using AVO analysis on the Blackfoot 3C-3D seismic data, southern Alberta, Canada: Geophysics, **67**, 27–37.

[6]. Fatti, J.L., Smith, G.C., Vail, P.L., Strauss, P.J., and Levitt, P.R. (1994): Detection of gas in sandstone reservoirs using AVO analysis: A 3-D seismic case history using the Geostack technique: Geophysics, 59, 1352- 1376.

[7]. Gassmann, F., (1951): Uber die elastizitatporosermedien: In G. Mavko, T. Mukerji, and J. Dvorkin eds., The Rock Physics Handbook: Tools for seismic analysis in porous media. Cambridge Univ. Press, 162-176.

[8]. Goodway, B., T. Chen, and J. Downton, (1997): Improved AVO fluid detection and lithology discrimination using Lame petrophysical parameters; 'λρ', 'μρ', & 'λ/μ fluid stack' from P and S inversions: 67th Annual International Meeting, SEG, Expanded Abstracts, 183-186.

[9]. Han, D. H., Q. Yao, and H. Z. Zhao,(2007): Complex properties of heavy oil sand: 77th Annual International Meeting, SEG, Expanded Abstracts, 1609–1613

[10]. Ostrander, W. J., (1984): Plane-wave reflection coefficients for gas sands at non-normal angles of incidence: Geophysics, **49**, 1637–1648.

[11]. Pendrel J., (2006): Seismic inversion- A critical tool in reservoir characterization: Scandinavian oil-gas magazine, 5/6, 19-22.

[12]. Quakenbush, M., Shang, B., and Tutle, C., (2006): Poisson impedance: The Leading Edge 25, 128-139

[13]. Russell, B.H., Hedlin, K., Flilterman, F.J., and Lines, L.R., (2003): Fluid-property discrimination with AVO: A Biot-Gassmann perspective: Geophysics, 68, 29-39.

[14]. Shuey, R.T., (1985), A simplification of the Zoeppritz equations: Geophysics, 50, 609- 614.

[15]. Smith, G.C., and Gidlow, P.M., (1987): Weighted stacking for rock property estimation and detection of gas: Geophysical prospecting, 35, 993- 1014.

[16]. Sayers, C., and S. Chopra, 2009, Special session: Rock physics: *The Leading Edge*, p.15-16.

[17]. Tuttle, M.L.W., Charpentier, R.R., and Brownfield, M.E., (1999): The Niger Delta petroleum system: Niger Delta province, Cameroon, and Equatorial Guinea, Africa: http://greenwood.cr.us gs. gov/energy/ Won dEnergy/O F99-5 0H/ChapterA.htm#TOP

[18]. Udo, K.I.; Akpabio, I.O; and Umoren, E.B (2017): Derived Rock Attributes Analysis for Enhanced Reservoir Fluid and Lithology Discrimination; *IOSR Journal of Applied Geology and Geophysics (IOSR-JAGG) e-ISSN: 2321–0990, p-ISSN: 2321–0982.Volume 5, Issue 2 Ver. I (Mar. - Apr. 2017), PP 95-105 www.iosrjournals.org*